Proceedings of the ASME 2019 38th International Conference on Ocean, Offshore and Arctic Engineering
OMAE2019
June 9-14, 2019, Glasgow, Scotland, UK

OMAE2019-95197

AN ENERGY-MAXIMISING MPC SOLUTION TO THE WEC CONTROL COMPETITION

Paolino Tona*, Guillaume Sabiron, Hoai-Nam Nguyen
IFP Energies nouvelles
Rond-point de l'échangeur de Solaize
BP 3, 69360 Solaize, France
Email: paolino.tona@ifpen.fr, guillaume.sabiron@ifpen.fr, hoai-nam.nguyen@ifpen.fr

ABSTRACT

The WEC Control Competition is a benchmark devised to compare energy-maximising controllers for wave energy converters, first in simulation, then in real time, using a scale device in a tank test situation. For the first round of the competition, the evaluators have provided a model of a leg of a Wavestar-like device, in the WEC-Sim simulation environment. The evaluation is based on an energy-related criterion computed on six irregular waves.

IFPEN's solution is an energy-maximising model predictive control (MPC), composed of an estimation algorithm for wave excitation force moment, using measurements (or estimations) of float displacement and velocity and PTO moment; an algorithm for short-term wave force prediction from present and past wave excitation force estimates, where no information about wave elevation is used; a real-time compatible MPC algorithm using wave force prediction, which maximises the average produced electric energy, taking into account the nonlinear PTO efficiency law.

INTRODUCTION

This paper describes the solution submitted by IFP Energies nouvelles (IFPEN) to the first round of the WEC Control Competition (WECCCOMP), a benchmark devised to compare energy-maximising controllers for wave energy converters (WECs), first in simulation, then in real time, using a scale device in a tank test situation [1].

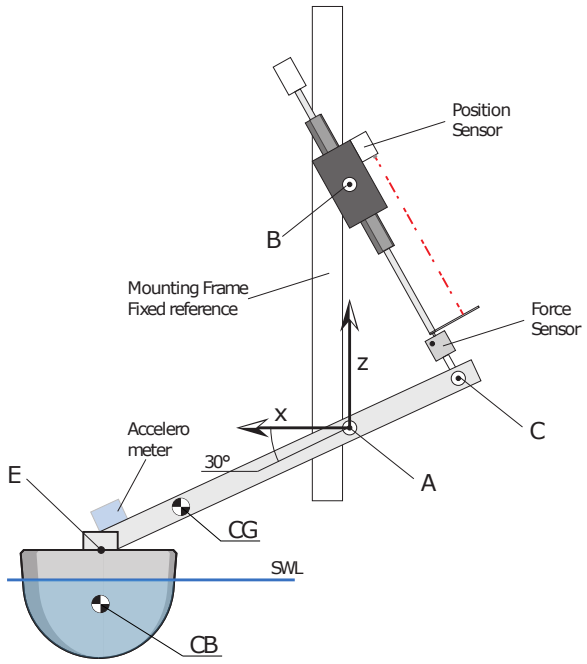

FIGURE 1. DIAGRAM OF EXPERIMENTAL WEC SYSTEM (FROM [1])

The benchmark focuses on a section of a Wavestar-like device (Figure 1), currently used for educational and research purposes at Aalborg University in Denmark. With a diameter of 25 cm, its float is at 1:20 scale with respect to the well-known pro-

*Address all correspondence to this author.

Copyright © 2019 ASME

totype deployed between 2009 and 2014 at Hanstholm (also in Denmark).

For the first round of the benchmark, the evaluators have developed a model of the scale device (Figure 1), coded in WEC-Sim, in which the contestants have integrated their controllers. An energy-related criterion was provided, to be computed on the results of simulations run on a set of six irregular waves.

Similar Wavestar-like setups have been the focus of research on WEC modelling and control, see for instance [2–4]. In particular, in [4], the authors present an experimental assessment of an energy-maximising model predictive controller taking into account PTO efficiency. The results of the 2015 test campaign in Aalborg wave basin were encouraging in terms of energy harvesting: the MPC controller fared much better than the PI controllers specifically tuned by Wavestar for each of the four sea states involved in the tests. However, the validation was only partially achieved, due to some relevant discrepancies between the simulation setup used to tune the MPC controller and the experimental setup. In fact, the PTO control loop, which had to be detuned to cope with friction in the hinge, turned out to have a greater impact on the overall dynamic behaviour than expected.

The WECCCOMP competition represents a good opportunity for IFPEN to further study the performance of the energy-maximising MPC control solution tested in 2015 and its suitability for this kind of WEC. Thus, the same control design approach as in [4], with minor adaptations, has been followed and proposed as a solution to the benchmark.

The different blocks of IFPEN model predictive control (MPC) system, are:

(a) An online estimation algorithm for wave excitation force (moment), using measurements (or estimations) of float displacement and velocity and PTO force (moment). The algorithm is based on a Kalman filter coupled with a random-walk model of the wave excitation force.
(b) An algorithm for short-term wave force prediction (1-5 s at full scale) from present and past wave excitation force estimation values, based on a nonlinear multi-step ahead error minimisation cost function, where an extended Kalman filter is used to solve the nonlinear optimisation problem. No information about wave elevation is used.
(c) A real-time compatible model predictive control algorithm using wave force prediction, which maximises the average produced electric energy, taking into account the nonlinear PTO efficiency law. The algorithm is based on the discretisation of the energy-maximising criterion via the trapezoidal method and the introduction of an equivalent discrete objective function where the instantaneous power values over the prediction horizon are weighted. The weightings are chosen offline using an iterative optimisation procedure.

The WEC model used for the design of algorithms (a) and (c) is an equivalent equation-of-motion (EoM) model, in the form of a fourth-order linear state-space representation, computed around the arm rotation point, using information given in [1] and data from the hydrodynamic database used to parameterise the WEC-Sim simulation.

With respect to the original approach in [4], a second offline optimisation step for the MPC controller has been added in order to find a local maximum for the evaluation criterion (which is not purely energetic) in the vicinity of the optimal solution which maximises electric energy production for the selected sea states. Three sets of weightings have been obtained, one for each pair of sea-states with the same significant wave height and peak period (but different peakedness factors). The appropriate set of weightings (or the corresponding set of QP parameters) is selected automatically online using a wave "recognition" procedure at the beginning of the simulation, based on the filtered estimation of the dominant wave frequency. The underlying algorithm, based on an unscented Kalman filter (UKF), is described in [5].

The paper is structured as follows. Section 1 recalls the main features of the benchmark setup. The control approach is explained in section 2. In Section 3, modelling issues are discussed, both for simulation and control design. Section 4 and section 5 present the results obtained respectively on the linear EoM model used for control design and on the WECCCOMP simulator. The last section summarises the conclusions and proposes further stages of research to improve the results in simulation and properly prepare for the experimental phase of the benchmark.

1 BENCHMARK SETUP

1.1 REFERENCE SETUP

The target WEC system comprises a float mechanically hinged at a fixed reference point (see Figure 1).

As the float is constrained to a circular motion in the plane $x-z$, the number of degrees of freedom of the device, from the PTO point of view, is reduced to just one. The PTO is a linear motor acting on the rotating arm, which can be force-controlled in both generator and motor mode, with setpoints possibly inducing reactive power terms.

The available sensors are the accelerometer and the position and force sensors depicted in Figure 1, plus 3 wave gauges measuring sea surface elevations upwave of the float.

1.2 SIMULATION MODEL

A numerical model of the Wavestar-like device is to be used for the development and the validation of the controllers submitted to the first stage of the competition. The simulation model has been implemented in WEC-Sim, an open-source code jointly developed by Sandia National Laboratories (Sandia) and the National Renewable Energy Laboratory (NREL) [6]. WEC-Sim is developed in MATLAB/Simulink, using Simscape Multibody to

Copyright © 2019 ASME

solve for a WEC's rigid body dynamics. The dynamic response of the modelled device is calculated by solving the WEC's equation of motion for each rigid body about its center of gravity in six degrees of freedom (DOF) based on Cummins' equation [7]:

$$(\mathbf{m}+\mathbf{A}_\infty)\ddot{\mathbf{X}} = -\int_0^t \mathbf{h_r}(t-\tau)\dot{\mathbf{X}}(\tau) + \mathbf{F_{ex}} + \mathbf{F_{vis}} + \mathbf{F_{hs}} + \mathbf{F_{PTO}} + \mathbf{F_m} \tag{1}$$

where $\mathbf{A}_\infty$ is the added mass at infinite frequency, $\mathbf{X}$ is the body displacement, $\mathbf{m}$ is the mass, $\mathbf{h_r}$ is the radiation impulse response function, $\mathbf{F_{ex}}$ is the wave excitation force, $\mathbf{F_{pto}}$ is the force from the PTO system, $\mathbf{F_{vis}}$ is the quadratic viscous drag term, $\mathbf{F_{hs}}$ is the hydrostatic restoring force, and $\mathbf{F_m}$ is the mooring force. The body displacement and the forces have six components each.

The WECCCOMP model includes the float's hydrodynamic response, described by an EoM in the form (1), as well as the physical linkages and joints represented in Figure 1. More precisely, the EoM does not include the mooring force (as there are no mooring lines), nor the quadratic viscous drag term (considered negligible with respect to the other forces). A linear wave-body interaction is assumed for the wave excitation force, which is precomputed by WEC-Sim before each simulation using the wave elevation as an input, as well as for the other terms. Thus, the only nonlinearities considered in the numerical model are due to the physical linkages and joints, between the float and the PTO.

Nonlinear transformations, included in the `Controller` block, allow to implement a "rotary controller" as in [2–4], that is a controller that computes setpoints for the equivalent pitch moment at the hinge point A (to be delivered by the linear motor acting as a PTO), using the float pitch angular position θ and acceleration $\ddot{\theta}$, computed from the accelerometer and the linear motor position sensor. The equivalent pitch moment applied by the PTO is also made available, from the linear motor force sensor. Note that the moment applied by the PTO differs from the setpoint because of the dynamics of the low-level linear motor controller, which is described by an experimentally identified discrete-time transfer function (with a 1.0 ms sample time, the same as the base sample time of the Simulink model).

1.3 OPERATING CONDITIONS AND EVALUATION CRITERIA

A series of six sea states, generated using the JONSWAP spectrum with the parameters given in Table 1, is employed in the evaluation.

For each sea state, the simulation lasts 100 dominant periods (that is, 98.8, 141.2 or 183.6 s, depending on T_p), with the first 25 seconds being discarded in the evaluation.

The following criterion, *EC*, is used to evaluate the controllers [1, 8] :

	S1	S2	S3	S4	S5	S6
H_{m0} [cm]	2.08	6.25	10.42	2.08	6.25	10.42
T_p [s]	0.988	1.412	1.836	0.988	1.412	1.836
γ [-]	1	1	1	3.3	3.3	3.3

TABLE 1. JONSWAP SPECTRA PARAMETERS FOR THE EVALUATION SEA STATES (SIGNIFICANT HEIGHT H_{M0}, DOMINANT PERIOD T_P, "PEAKEDNESS" FACTOR γ

$$EC(P,f,z) = \frac{\text{avg}(P)}{2 + \frac{|f|_{98}}{F_{max}} + \frac{|z|_{98}}{Z_{max}} - \frac{\text{avg}|P|}{P_{98}}} \tag{2}$$

where:

- avg(P) ($\overline{P}$ in the following) is the average absorbed electrical power (in W);
- $|f|_{98}$ is the 98th percentile of the absolute PTO force time history (in N);
- F_{max} is the force constraint on the PTO (60 N);
- $|z|_{98}$ is the 98th percentile of the absolute displacement time history (in m);
- Z_{max} is the displacement constraint on the PTO (0.08 m)
- P_{98} is the 98th percentile of the absolute electrical power time history (in W);
- avg$|P|$ is the mean absolute electrical power (in W).

The electrical absorbed power is computed in post-processing after each sea-state simulation as follows:

$$P = \eta_{PTO} P_a, \quad \eta_{PTO} = \begin{cases} \eta \text{ if } P_a \geq 0 \\ 1/\eta \text{ if } P_a < 0 \end{cases} \tag{3}$$

where P_a is the linear motor absorbed mechanical power (given by the product of PTO force and PTO velocity), and $\eta = 0.7$.

Note that *EC* is defined in the linear reference frame of the PTO, not in the rotary reference frame. Note also that the overall evaluation criterion is obtained adding the scores for each sea state, with no weightings, which gives greater prominence to the results obtained with the most energetic waves (S3 and S6).

2 CONTROL DESIGN

The block diagram of IFPEN model predictive control system [4] is sketched in Figure 2.

Copyright © 2019 ASME

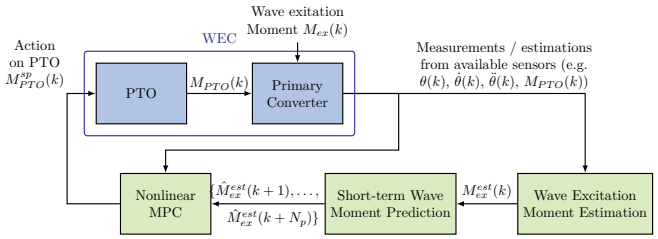

FIGURE 2. IFPEN MPC SYSTEM

As in most other research studies on Wavestar-like devices, a "rotary" controller framework is assumed, with the float rotational dynamics around the hinge point being described by state-space models derived from the equation of motion. Model inputs are M_{PTO} and M_{ex}, respectively the PTO moment and the wave excitation moment, while model outputs are θ and $\dot{\theta}$, respectively the float rotational displacement (with respect to the equilibrium point) and velocity. Float velocity can be easily estimated from position and acceleration measurements via a Kalman filter. On the real device, for a given sea state, the equivalent wave excitation moment around the hinge point can be computed offline in a dedicated experiment where the PTO is position-controlled to keep the float blocked against the wave action: the opposite of the recorded equivalent moment applied by the controller is then the wave excitation moment, according to the linear wave theory and Cummins equation. However, the wave excitation moment is not directly accessible during the normal device operation, which is the rationale behind the estimation block in Figure 2.

2.1 WAVE EXCITATION MOMENT ESTIMATION

In [9] an estimation algorithm for wave excitation force is proposed, using a combination of a bank of independent harmonic oscillators and a Luenberger observer. The strategy is tested on a real WEC system. However the reported experimental results show a relatively high phase lag in the estimated signal compared to the measured signal.

In [10], by considering the wave excitation force as a time-varying sinusoid, an extended Kalman filter (EKF) approach is presented. However, no experimental results are reported. In addition, the approach can clearly be effective only for very narrow-banded wave forces.

By combining several pressure sensors at discrete points on the buoy surface with the buoy heave position, and with an extended Kalman filter, another approach is proposed in [11]. However, the computational complexity may be high. In addition, additional pressure sensors are required.

The approach followed here and implemented in [4], has been developed to overcome the aforementioned drawbacks.

Its most important features are:

- only standard WEC measurements (position, velocity, PTO moment) are used by the algorithm;
- the experimental results in [4] show that estimated wave torque values do not have any significant lag compared to "true" values, which is not the case for the approach in [9];
- in contrast to [9], no (implicit) unrealistic assumption about the time-invariant nature of the sea state is made, hence any operating condition can be efficiently dealt with.

The underlying algorithm is based on a linear Kalman filter and a random walk model for the variation of the wave excitation moment and is fully described in [12].

The algorithm requires the calibration of three (diagonal) covariance matrices, for the initial state and the state and output noises. Note that as the algorithm does not require a sea-state specific calibration, it is run with the same set of parameters for S1 to S6. The sample time of the algorithm is 5 ms.

2.2 WAVE EXCITATION MOMENT PREDICTION

In the WECCCOMP context, given the availability of three wave gauges in front of the device, it is in principle possible to compute future values of the wave excitation moments from wave elevation predictions, using the impulse responses relating wave elevation to wave excitation force in the hydrodynamic database. Indeed, spatial prediction of wave elevation has drawn a lot of attention in the hydrodynamic control community [13–16]. However this approach requires a wave propagation model which can prove difficult to develop and lack robustness.

Another approach, that has become popular in the last years because of its simplicity, is to use past time series of local measurements or estimates, at the float position. In [17], using real wave elevation data, Fusco and Ringwood show that a relatively simple linear auto-regressive (AR) model can perform quite well, provided that the high-frequency content is filtered out from the time series data. To avoid introducing a phase lag, the use of a non-causal zero-phase filter is advocated. The solution is based on a *batch-processing* approach, which also includes a computationally-expensive nonlinear least squares problem to be solved and a spectral analysis to be performed in order to compute an optimal sampling period for all the computations. In [18], an iterative, more easily implementable approach is proposed, based on a bank of least squares estimators. However, it implicitly assumes that the sea state is constant.

The algorithm for wave excitation moment prediction implemented for WECCCOMP, fully described in [19], uses the estimates computed by the aforementioned wave excitation moment estimation algorithm. It is based on a nonlinear multi-step ahead error minimisation cost function. An extended Kalman filter (EKF) is used to solve the nonlinear optimisation problem, so the algorithm is recursive and easy to implement. As shown in [19], it automatically "adapts" the coefficients of the underlying AR model to the current sea-state. Once again, this algo-

Copyright © 2019 ASME

rithm does not require a sea-state specific calibration of the covariance matrices. For WECCCOMP, it has been implemented with a sample time of 50 ms, an AR-model order of 16 and a prediction horizon of 25 samples (that is 1.25 s). Thus, each 50 ms, a new vector of 25 prediction is generated and fed to the MPC algorithm.

2.3 ENERGY-MAXIMISING MODEL NONLINEAR PREDICTIVE CONTROL

The energy-maximising MPC algorithm experimentally evaluated in [4] has not been published yet in the literature, but its principle is described in the French patent [20]. The approach is based on the discretisation of the following (nonlinear) energy-maximising criterion:

$$\overline{P}(t) = \int_0^T P(t)dt = \int_0^T \eta_{PTO} P_a(t)dt = \int_0^T \eta_{PTO} M_{PTO}(t)\dot{\theta}(t)dt \tag{4}$$

When a bidirectional PTO is available, as it is the case for the WEC under study, it is paramount that PTO efficiency is considered to maximise electrical energy production, and not simply mechanical energy. With $\eta = 0.7$ in (3), to compensate for the electric power drawn from the grid in motor mode, twice more mechanical power is required in generator mode. While simple, the expression for PTO efficiency in (3) is nonlinear, and taking it into account generally leads to a non-convex criterion, whose optimisation in real time may prove difficult due to computational constraints [21].

In [4], the criterion (4) is discretised via the trapezoidal method (which improves the accuracy with respect to the standard discretisation method of the literature) and the introduction of an equivalent discrete objective function where the PTO moment – float velocity products (i.e, the instantaneous mechanical power values) over the prediction horizon are weighted. The weightings are chosen offline using an iterative optimisation procedure based on repeated simulations of the EoM model over a set of sea states (a Nelder-Mead optimisation algorithm is used). A modification of the eigenvalues of the quadratic matrix H of the MPC criterion in QP form ensures the strict convexity of the QP objective function, with a minimal loss of optimality compared to other convexification procedures (e.g., the introduction of a control weighting). In fact, this approach shifts the complexity of optimising the original non-convex criterion online to an offline optimisation procedure, which is not subject to real-time computational constraints.

In this study, with respect to the approach in [4], a second offline optimisation step for the MPC controller has been added in order to find a local maximum for the evaluation criterion (which is not purely energetic) in the vicinity of the optimal solution which maximises electric energy production for the selected sea states. Instead of having a single set of weightings (and corresponding QP parameters) as in [4], different sets have been computed. The ones used in the solution for the benchmark have been computed for the pairs S1–S4, S2–S5 and S3–S6. The appropriate set of weighting (or the corresponding set of QP parameters) is selected automatically online using a wave "recognition" procedure during the first 25 s of simulation, based on a filtered estimation of the dominant wave frequency. The underlying algorithm, based on an unscented Kalman filter (UKF), is described in [5].

The sample times of MPC and UKF are respectively 50 ms and 10 ms.

3 MODELING FOR CONTROL

For both wave excitation force estimation and MPC, the following model is used to describe the WEC dynamics:

$$\begin{cases} (J+J_\infty)\ddot{\theta}(t) &= -K_{hs}\theta(t) - M_r(t) + M_{ex}(t) - M_{PTO}(t) \\ \dot{r}(t) &= A_r r(t) + B_r \dot{\theta}(t), \\ M_r(t) &= C_r r(t) + D_r \dot{\theta}(t) \end{cases} \tag{5}$$

where:

- J_∞ is the (float + arm) mass moment of inertia;
- J is the added mass moment of inertia;
- K_{hs} is the hydrostatic coefficient;
- M_r is the radiation moment due to float velocity;
- $(A_r; B_r; C_r; D_r)$ are the matrices of a state-space realization in the variable $r(t)$, an internal state with no particular physical meaning, of the inconvenient convolution product $M_r(t) = \int_0^t h_{r,\dot{\theta}}(t-\tau)$, obtained using Prony's method.

with all the variables and parameters defined with respect to the rotation around hinge point A.

As mentioned before, this modelling approach had been followed in [4], though for a slightly different set-up (float orientation with respect to incoming waves, low-level PTO control and possibly float design). The parameters for model (5) had been provided by Wavestar based on experiments and on hydrodynamic database for the float, computed by WAMIT with respect to the hinge point. For the present study, no experimental data has been provided yet, so the calibration of (5) has been carried out using the WEC-Sim simulator (and its hydrodynamic database) as well as information provided in the competition description [1] and the dedicated forum. The corresponding parameters values are given in Table 2.

Note that, as no information is given about added inertia in [1], J_∞ has been retrieved as the pitch component of the float added inertia matrix (used in WEC-Sim), after it has been translated to the hinge point from the reference point used in WAMIT to compute the hydrodynamic database. Note also that, as the developers of the WEC-Sim model have introduced a linear damping coefficient (denoted k_{ls}) of $1.8\,\mathrm{N\,m\,rad^{-1}\,s^{-1}}$ on $\dot{\theta}$ to improve

Copyright © 2019 ASME

HYDRODYNAMIC MODEL PARAMETERS		
Inertia of arm and float	J	$1.0\,\mathrm{kg\,m^2}$
Hydrostatic stiffness coefficient	K_{hs}	$92.33\,\mathrm{N\,m\,rad^{-1}}$
Added inertia	J_∞	$0.4805\,\mathrm{kg\,m^2}$
RADIATION MOMENT IMPULSE RESPONSE REALIZATION		
$A_r = \begin{bmatrix} -13.59 & -13.35 \\ 8.0 & 0 \end{bmatrix}, \quad B_r = \begin{bmatrix} 8.0 \\ 0 \end{bmatrix}$		
$C_r = \begin{bmatrix} 4.739 & 0.5 \end{bmatrix}, \quad D_r = -0.1586$		

TABLE 2. PARAMETER VALUES FOR DESIGN MODEL

the fit to experimental data, in the final model the same coefficient has been added to D_r, defined in Table 2.

The resulting design model is a 4th-order linear state-space representation and is expressed as follows:

$$A_c = \begin{bmatrix} 0 & 1 & \mathbf{0}_{1\times 2} \\ -\frac{K_{hs}}{J+J_\infty} & -\frac{D_r+k_{ls}}{J+J_\infty} & -\frac{C_r}{J+J_\infty} \\ 0 & B_r & A_r \end{bmatrix},$$
$$B_c = \begin{bmatrix} 0 \\ \frac{1}{J+J_\infty} \\ \mathbf{0}_{2\times 1} \end{bmatrix}, \; C_c = \begin{bmatrix} 1 & 0 & \mathbf{0}_{1\times 2} \\ 0 & 1 & \mathbf{0}_{1\times 2} \end{bmatrix}$$

where $\mathbf{0}_{m\times n}$ is a zero matrix with m rows and n columns.

3.1 MODEL ASSESSMENT

A way to check the validity of the design model, is to compare its outputs (float rotational position and velocity), for each sea-state,with no control applied, to the outputs provided by the WECCCOMP simulator. This requires the computation of the wave excitation moment w.r.t. the hinge point A, to be used as input to the design model. For each sea state, M_{ex} has been computed following four different approaches:

- from the wave elevation, via the impulse responses computed from the hydrodynamic database for heave, surge and pitch, as

$$M_{ex}^{hyd} = F_{ex,x}\sin(\theta_0)l_{arm} - F_{ex,z}\cos(\theta_0)l_{arm} + M_{ex,\theta} \qquad (6)$$

  where θ_0 is the pitch equilibrium position, l_{arm} the arm length, $F_{ex,x}$, $F_{ex,z}$ and $M_{ex,\theta}$ the components of the wave excitation force acting on the float in the surge, heave and pitch directions;
- as the opposite of the PTO moment applied by a (specifically designed) controller to keep the float blocked, mimicking the experimental procedure (M_{ex}^{exp});
- from (6) $F_{ex,x}$, $F_{ex,z}$ and $M_{ex,\theta}$ computed by WEC-Sim along the simulation and (M_{ex}^{sim,θ_0});
- using (6), but with the varying θ obtained from the WEC-Sim simulation ($M_{ex}^{sim,\theta}$).

The latter is supposed to be the "true" wave excitation moment, taking into account the nonlinearities due to the rotation around the hinge point.

Table 3 and Table 4 show the cross goodness-of-fit computed as a normalized root mean square (NRMS) measure, between the different computed moments, for S1 and S6 respectively.

	$M_{ex}^{sim,\theta}$	M_{ex}^{sim,θ_0}	M_{ex}^{exp}	M_{ex}^{hyd}
$M_{ex}^{sim,\theta}$	1	0.98	0.99	0.97
M_{ex}^{sim,θ_0}	0.98	1	0.99	0.97
M_{ex}^{exp}	0.99	0.99	1	0.97
M_{ex}^{hyd}	0.97	0.97	0.97	1

TABLE 3. CROSS (NRMS) GOODNESS-OF-FIT BETWEEN COMPUTED WAVE EXCITATION MOMENTS FOR S1 (WITHOUT CONTROL)

	$M_{ex}^{sim,\theta}$	M_{ex}^{sim,θ_0}	M_{ex}^{exp}	M_{ex}^{hyd}
$M_{ex}^{sim,\theta}$	1	0.92	0.92	0.92
M_{ex}^{sim,θ_0}	0.92	1	0.99	0.97
M_{ex}^{exp}	0.92	0.99	1	0.98
M_{ex}^{hyd}	0.92	0.97	0.98	1

TABLE 4. CROSS (NRMS) GOODNESS-OF-FIT BETWEEN COMPUTED WAVE EXCITATION MOMENTS FOR S1 (WITHOUT CONTROL)

Note that M_{ex}^{exp} and M_{ex}^{hyd}, corresponding to the only two computation methods available "in real life", are very close to each other and to M_{ex}^{sim,θ_0}, the wave excitation moment around the equilibrium point θ_0 computed via WEC-Sim. However, when the float moves far from θ_0 as it happens with the most energetic waves , the "true" wave excitation moment is shifted with respect to those computed around θ_0, as shown in Figure 3.

Copyright © 2019 ASME

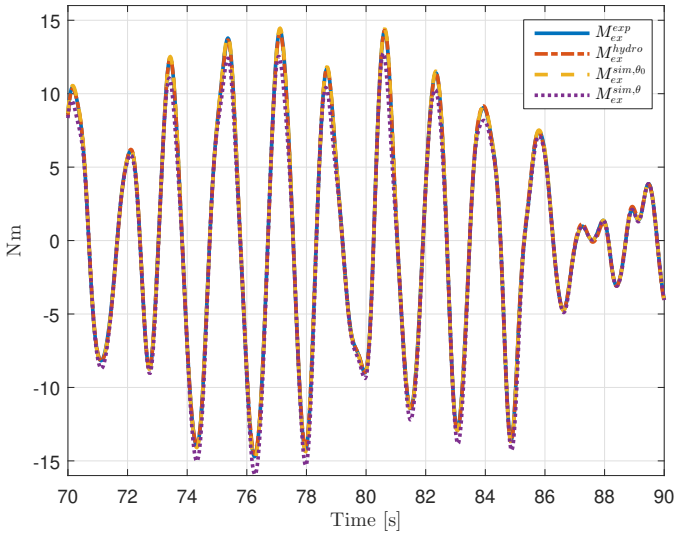

FIGURE 3. COMPUTED WAVE EXCITATION MOMENT FOR S6 (WITHOUT CONTROL)

		S1	S2	S3	S4	S5	S6
Design model	θ GoF	0.92	0.91	0.82	0.92	0.91	0.81
	$\dot{\theta}$ GoF	0.92	0.89	0.76	0.92	0.88	0.71
ID model 1	θ GoF	0.97	0.97	0.83	0.97	0.92	0.82
	$\dot{\theta}$ GoF	0.98	0.91	0.77	0.97	0.89	0.73
ID model 2	θ GoF	0.84	0.89	0.84	0.89	0.90	0.82
	$\dot{\theta}$ GoF	0.83	0.87	0.78	0.87	0.87	0.74

TABLE 5. NRMS GOODNESS-OF-FIT (GOF) FOR DESIGN MODEL AND TWO IDENTIFIED MODELS FOR ALL THE SEA STATES (WITHOUT CONTROL)

$M_{ex}^{sim,\theta}$ time series recorded from WEC-Sim have been used as inputs for the design model to check its capacity to reproduce WEC behaviour as simulated by WEC-Sim, for the no control (free-float) case.

Table 5 shows the NRMS goodness-of-fit (GoF) obtained with the design model for all the sea states, in the no-control case. In the same table, GoF measures are also given for two 4^{th}-order free-structure continuous state-space models identified with the PEM method of Matlab's System Identification Toolbox, the first using inputs and outputs of the simulation with S1 only, and the second, a concatenation of all the sea states. The results with the identified models suggest that the design model could be improved, via a grey-box system identification procedure for instance, but only marginally for the most energetic waves.

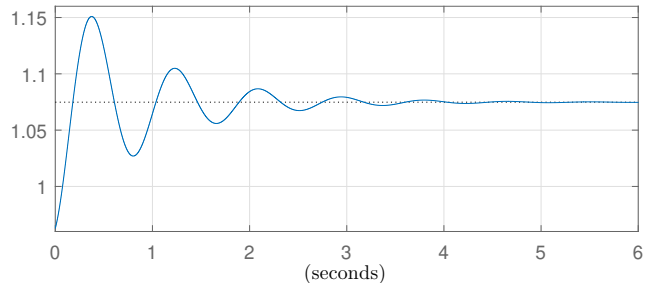

FIGURE 4. PTO CONTROLLER STEP RESPONSE

In view of the experimental implementation, the IFPEN team has decided not to try to match at all cost the design model to a simulation model which is not perfect, either. Let us recall that the WEC-Sim model does not include any nonlinear wave-float interaction, be it for the hydrostatic force or for the Froude-Krylov excitation force, whose introduction may improve the fit with the experimental results (as shown, for instance, in [3]). In fact, the validation results of the WECCCOMP numerical model described in [8], clearly show that the model tends to overestimate the float motion over the range of frequency of interest.

3.2 PTO MODEL

In the experimental campaign described in [4], it had been found out that the dynamics of the PTO servo controller, which had been slowed down to cope with mechanical friction in the device, had a significant impact on the overall performance of both MPC and PI control. A second round of offline optimisations run with the WEC model together with a linear approximation of WEC dynamics was required to increase the performance. Since then, the MPC algorithm has been improved by including PTO dynamics, if available, directly in the design model, which gives better results than simply calibrating the weightings in the presence of this dynamics.

The step response of experimentally identified dynamics of the PTO controller is shown in Figure 4. It can be noticed that it has a direct term (the transfer function is non strictly proper) and a non-unitary DC gain, quite differently from the behaviour noted in [4]. According to the organisers, this is because the force feedback control (considered too slow) has been replaced by a current feedforward control.

Unfortunately, this kind of dynamics cannot be easily included in MPC design, as it makes the resulting design model too stiff. Thus, PTO dynamics has only been taken into account by means of the weightings computed in the offline optimisation procedure.

Copyright © 2019 ASME

4 NOMINAL DESIGN AND RESULTS

As explained before, the MPC approach deployed for WEC-CCOMP requires an offline optimisation step, which iteratively adjusts the prediction weightings while maximising the energy criterion, by running a series of simulations on the design model. This step is carried out using a Simulink model which includes the blocks of Figure 2, with the state-space realisation of (5) and the identified PTO transfer function representing the WEC dynamics. Starting from the weightings computed in this first step, which maximise $\overline{P}$, an additional optimisation is performed on the EC, computed from the rotary reference frame measurements using trigonometric transformations. As the EC is quite different from the original energy criterion maximised by the MPC, the second optimisation only aims at finding weightings which improve the EC (at the expense of $\overline{P}$), but not at finding a global maximum for it.

For each sea state, the input of the simulation is the theoretical wave excitation moment in M_{ex}^{hyd} computed from the hydrodynamic database in the rotary framework (6). M_{ex}^{exp} (or M_{ex}^{sim,θ_0}) could have been used instead. Knowing the wave excitation moment, and in the absence of noise, it is quite easy to calibrate the parameters of the wave moment estimation algorithm, which provides almost perfect estimates. It is a bit more difficult to calibrate the wave moment prediction algorithm in order to obtain accurate predictions over all the prediction horizon, but it can be shown (using the ideal case of perfect prediction as a benchmark) that a good accuracy for the first few prediction steps suffices. Concerning the MPC, as the QP matrices are chosen, via the weightings, by the iterative optimisation procedure, there is one calibration parameter left: M_{max}, the moment constraint on the PTO. In fact, the linear force constraint $F_{max} = 60\,\mathrm{N}$ in the EC does not map to a fixed value in the rotary reference frame. For the expected range of motion, depending on θ, the resulting PTO moment is comprised between approximately $10\,\mathrm{N\,m}$ and $12\,\mathrm{N\,m}$. Conservatively, a value of $10\,\mathrm{N\,m}$ has been chosen.

Weightings (and QP matrices) have been computed for the sea-state pairs S1–S4, S2–S5 and S3–S6 both for $\overline{P}$ and EC. In fact, while it is possible to compute a specific set of parameters for each wave individually, it seems difficult in practice to discriminate (on line) two waves with the same peak period and significant height.

The results are shown in Table 6 together with the results obtained using a PI controller with a set of gains computed, using again the Nelder-Mead optimisation algorithm, so as to maximise $\overline{P}$ for each sea state being simulated, while applying the same constraints on PTO moment as the MPC. MPC improves both criteria of up to 20% with respect to PI for waves S3 and S6 that contains the higher power capacity. Values were rounded to nearest milliwatt for clarity.

	Metric	S1	S2	S3	S4	S5	S6
$\mathrm{PI}_{\overline{P}}$	$\overline{P}$ [mW]	15	207	593	21	236	612
	EC [mW/-]	8	81	183	11	87	185
$\mathrm{MPC}_{\overline{P}}$	$\overline{P}$ [mW]	16	233	708	23	263	728
	EC [mW/-]	8	89	219	11	95	221
MPC_{EC}	$\overline{P}$ [mW]	16	228	706	23	254	730
	EC [mW/-]	8	92	221	11	97	223

TABLE 6. SIMULATION RESULTS ON LINEAR SYSTEM FOR $\mathrm{PI}_{\overline{P}}$, $\mathrm{MPC}_{\overline{P}}$ AND MPC_{EC}

5 IMPLEMENTATION IN WEC-SIM AND RESULTS

The control blocks used for the calibration phase have been directly copied and pasted inside the `Controller` block of the WEC-Sim simulator, without any modification. A Kalman filter is added to estimate float velocity, which is not measured in the simulator (nor in the real device), from float position and acceleration.

The calibration of each control block is the same as in the design model simulations. Regarding the wave estimation algorithm, a trade-off could have been made on its calibration to make it less aggressive than in the linear simulation to take into account the design model – WEC-Sim model mismatch.

It can be noticed from Figure 5 which compares the output of the wave estimation algorithm to $M_{ex}^{sim,\theta}$ computed via WEC-Sim, that there are significant estimation errors, in particular when the control saturates. The errors are larger for the most energetic waves (inducing wider ranges of motion) which suggests that the design model is not representative enough. Overall, the wave estimation results are considerably worse than those obtained in the experimental tests of [4]. Hopefully, the second phase of WECCCOMP will help clarify if these results depend on the modelling choices in WEC-Sim or on the inadequacy of the linear design model.

Table 7 shows the results obtained on WEC-Sim in terms of $\overline{P}$ and EC, with the MPC weightings and the PI gains computed with the design model. The improvements provided by the MPC are smaller than in the simulations with the design model, but can be still considered significant for the most energetic waves with increases in terms of EC of up to 15% (for S6).

6 CONCLUSIONS AND PERSPECTIVES

At the time of writing, the analysis of the results is still underway. The performance of the wave estimation algorithm and of the MPC is somewhat disappointing, especially compared to previous experimental results obtained with a similar setup.

Copyright © 2019 ASME

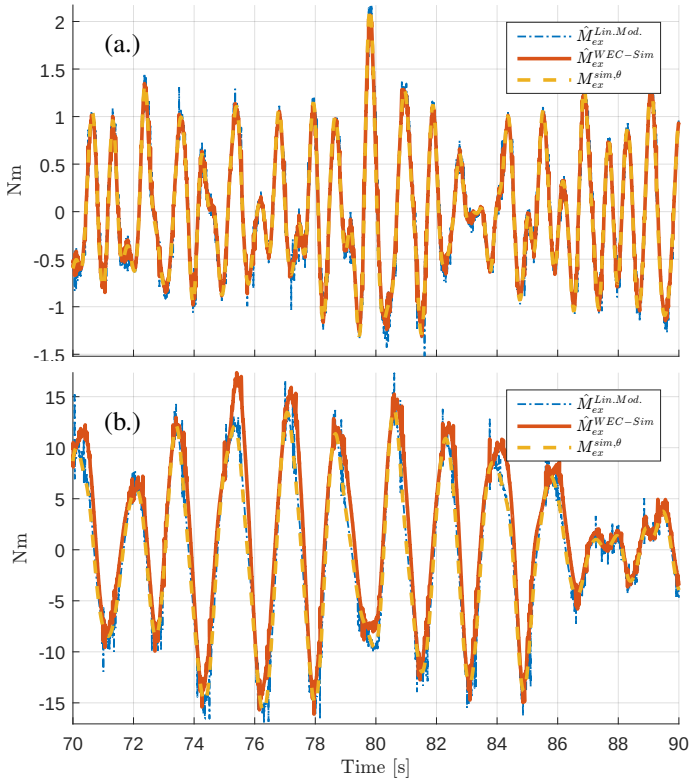

FIGURE 5. COMPARISON BETWEEN OUTPUT OF THE WAVE ESTIMATION ALGORITHM TO $M_{EX}^{SIM,\theta}$ COMPUTED VIA WEC-SIM FOR WAVES S1 (a.) AND S6 (b.)

	Metric	S1	S2	S3	S4	S5	S6
$PI_{\overline{P}}$	$\overline{P}$ [mW]	14	192	556	19	213	590
	EC [mW/-]	7	76	172	10	80	177
$MPC_{\overline{P}}$	$\overline{P}$ [mW]	15	207	614	20	227	663
	EC [mW/-]	8	79	191	10	82	202
MPC_{EC}	$\overline{P}$ [mW]	15	207	618	20	225	662
	EC [mW/-]	8	84	194	10	86	204

TABLE 7. SIMULATION RESULTS ON WEC-SIM ENVIRONMENT FOR $PI_{\overline{P}}$, $MPC_{\overline{P}}$ AND MPC_{EC}

However, while similar, the new setup does differ in terms of range of motion and PTO dynamics. It remains to be seen how these differences affect the practical performance of the proposed controller and whether a new MPC design which directly takes into account the PTO dynamics in the nominal model would be able to improve the results. Hopefully, the second phase of WEC-CCOMP will provide more insight.

REFERENCES

[1] Ringwood, J., Ferri, F., Ruehl, K., Yu, Y.-H., Coe, R., Bacelli, G., Weber, J., and Kramer, M., 2017. "A competition for WEC control systems". In Proceedings of the 12th European Wave and Tidal Energy Conference (EWTEC).

[2] Jakobsen, M. M., Ferri, F., and Kramer, M. M., 2015. "Control of point absorbers and their performance in experiments". In Proceedings of the 11th European Wave and Tidal Energy Conference (EWTEC).

[3] Zurkinden, A., Ferri, F., Beatty, S., Kofoed, J., and Kramer, M., 2014. "Non-linear numerical modeling and experimental testing of a point absorber wave energy converter". *Ocean Engineering,* ***78***, pp. 11 – 21.

[4] Nguyen, H., Sabiron, G., Tona, P., Kramer, M., and Vidal-Sanchez, E., 2016. "Experimental validation of a nonlinear MPC strategy for a wave energy converter prototype". In ASME 2016 35th International Conference on Ocean, Offshore and Arctic Engineering, Vol. 6, American Society of Mechanical Engineers.

[5] Nguyen, H.-N., Tona, P., and Sabiron, G., 2017. "Dominant wave frequency and amplitude estimation for adaptive control of wave energy converters". In ASME 2017 36th International Conference on Ocean, Offshore and Arctic Engineering, OCEANS 2017 - Aberdeen, pp. 1 – 6.

[6] Lawson, M., Yu, Y.-H., Ruehl, K., and Michelen, C., 2014. "Development and demonstration of the WEC-Sim wave energy converter simulation tool". In Proceedings of the 2nd Marine Energy Technology Symposium (METS 2014).

[7] Cummins, W., 1962. The impulse response function and ship motions. Tech. rep., DTIC Document.

[8] Tom, N., Ruehl, K., and Ferri, F., 2018. "Numerical model development and validation for the WECCCOMP control competition". In ASME 2018 37th International Conference on Ocean, Offshore and Arctic Engineering, American Society of Mechanical Engineers.

[9] Kracht, P., Perez-Becker, S., Richard, J.-B., and Fischer, B., 2015. "Performance improvement of a point absorber wave energy converter by application of an observer-based control: Results from wave tank testing". *IEEE Transactions on Industry Applications,* ***51***(4), pp. 3426–3434.

[10] Ling, B., and Batten, B., 2015. "Real time estimation and prediction of wave excitation forces on a heaving body". In SME. International Conference on Offshore Mechanics and Arctic Engineering, Volume 9: Ocean Renewable Energy.

[11] Abdelkhalik, O., Zou, S., Robinett, R., Bacelli, G., and Wilson, D., 2016. "Estimation of excitation forces for wave energy converters control using pressure measurements". *International Journal of Control*, pp. 1–13.

[12] Nguyen, H.-N., and Tona, P., 2017. "Wave excitation force estimation for wave energy converters of the point absorber

Copyright © 2019 ASME

type". *IEEE Transactions on Control System Technology*. (submitted for publication).

[13] Tedd, J., and Frigaard, P., 2007. "Short term wave forecasting, using digital filters, for improved control of wave energy converters". In Proc. of Int. Offshore and Polar Eng. Conf, Vol. 388, p. 394.

[14] Serafino, F., Lugni, C., and Soldovieri, F., 2010. "A novel strategy for the surface current determination from marine x-band radar data". *IEEE Geoscience and Remote Sensing Letters,* ***7***(2), pp. 231–235.

[15] Paparella, F., Monk, K., Winands, V., Lopes, M., Conley, D., and Ringwood, J. V., 2015. "Up-wave and autoregressive methods for short-term wave forecasting for an oscillating water column". *IEEE Transactions on Sustainable Energy,* ***6***(1), pp. 171–178.

[16] Belmont, M., Horwood, J., Thurley, R., and Baker, J., 2006. "Filters for linear sea-wave prediction". *Ocean Engineering,* ***33***(17), pp. 2332–2351.

[17] Fusco, F., and Ringwood, J. V., 2010. "Short-term wave forecasting for real-time control of wave energy converters". *Sustainable Energy, IEEE Transactions on,* ***1***(2), pp. 99–106.

[18] Fischer, B., Kracht, P., and Perez-Becker, S., 2012. "Online-algorithm using adaptive filters for short-term wave prediction and its implementation". In Proceedings of the 4th International Conference on Ocean Energy (ICOE), Dublin, Ireland (Vol. 1719)., pp. 17–19.

[19] Nguyen, H.-N., and Tona, P., 2018. "Short-term wave force prediction for wave energy converter control". *Control Engineering Practice,* ***75***, pp. 26 – 37.

[20] Nguyen, H.-N., and Tona, P., 2018. PROCEDE DE COMMANDE D'UN SYSTEME HOULOMOTEUR AU MOYEN D'UNE COMMANDE OBTENUE PAR MINIMISATION D'UNE FONCTION OBJECTIF PONDEREE ET DISCRETISEE PAR LA METHODE DES TRAPEZES. French patent n. 3058476, 11 May 2018.

[21] Tona, P., Nguyen, H.-N., Sabiron, G., and Creff, Y., 2015. "An efficiency-aware model predictive control strategy for a heaving buoy wave energy converter". In Proceedings of the 11th European Wave and Tidal Energy Conference (EWTEC).

Copyright © 2019 ASME